

A multicenter evaluation of a new post-processing method with depth-dependent collimator resolution applied to full-time and half-time acquisitions without and with simultaneously acquired attenuation correction

Carmelo V. Venero, MD,^a Gary V. Heller, MD, PhD, FACC,^{a,b}
Timothy M. Bateman, MD, FACC,^{c,d} A. Iain McGhie, MD, FACC,^c
Alan W. Ahlberg, MA,^a Deborah Katten, RN,^a Staci A. Courter, MA,^d
Robert J. Golub, MD, FACC,^e James A. Case, PhD,^d and S. James Cullom, PhD^d

Background. The field of nuclear cardiology is limited by image quality and length of procedure. The use of depth-dependent resolution recovery algorithms in conjunction with iterative reconstruction holds promise to improve image quality and reduce acquisition time. This study compared the Astonish algorithm employing depth-dependent resolution recovery and iterative reconstruction to filtered backprojection (FBP) using both full-time (FTA) and half-time (HTA) data. Attenuation correction including scatter correction in conjunction with the Astonish algorithm was also evaluated.

Methods. We studied 187 consecutive patients (132 with cardiac catheterization and 55 with low likelihood for CAD) from three nuclear cardiology laboratories who had previously undergone clinically indicated rest/stress Tc-99m sestamibi or tetrofosmin SPECT. Acquisition followed ASNC guidelines (64 projections, 20-25 seconds). Processing of the full-time data sets included FBP and Astonish (FTA). A total of 32 projection data sets were created by stripping the full-time data sets and processing with Astonish (HTA). Attenuation correction was applied to both full-time and half-time Astonish-processed images (FTA-AC and HTA-AC, respectively). A consensus interpretation of three blinded readers was performed for image quality, interpretative certainty, and diagnostic accuracy, as well as severity and reversibility of perfusion and functional parameters.

Results. Full-time and half-time Astonish processing resulted in a significant improvement in image quality in comparison with FBP. Stress and rest perfusion image quality (excellent or good) were 85%/80% (FBP), 98%/95% (FTA), and 95%/92% (HTA), respectively ($p < 0.001$). Interpretative certainty and diagnostic accuracy were similar with FBP, FTA, and HTA. Left ventricular functional data were not different despite a slight reduction in half-time gated image quality. Application of attenuation correction resulted in similar image quality and improved normalcy (FTA vs. FTA-AC: 76% vs. 95%; HTA vs. HTA-AC: 76% vs. 100%) and specificity (FTA vs. FTA-AC: 62% vs. 78%; HTA vs. HTA-AC: 63% vs. 84%) ($p < 0.01$ for all comparisons).

Conclusion. Astonish processing, which incorporates depth-dependent resolution recovery, improves image quality without sacrificing interpretative certainty or diagnostic accuracy. Application of simultaneously acquired attenuation correction, which includes scatter

From Hartford Hospital,^a Hartford, CT; University of Connecticut,^b Farmington, CT; Mid America Heart Institute and University of Missouri-Kansas City,^c Kansas City, MO; Cardiovascular Imaging Technologies,^d Kansas City, MO; and Cardiology Associates of Central Connecticut,^e Wallingford, CT.

This research was supported in part by an unrestricted clinical research grant from Philips Medical Systems, Milpitas, CA.

Received for publication Dec 10, 2008; final revision accepted May 26, 2009.

Reprint requests: Gary V. Heller, MD, PhD, FACC, Hartford Hospital, 80 Seymour Street, Hartford, CT 06102; gheller@harthosp.org. 1071-3581/\$34.00

Copyright © 2009 by the American Society of Nuclear Cardiology. doi:10.1007/s12350-009-9106-9

correction, to full-time and half-time images processed with this method, improves specificity and normalcy while maintaining high image quality. (*J Nucl Cardiol* 2009;16:714-25.)

Key Words: Attenuation and scatter correction • instrumentation: SPECT • myocardial perfusion imaging: SPECT • image processing • ischemia • myocardial

INTRODUCTION

Stress SPECT myocardial perfusion imaging (MPI) has become an important test for assessing patients with suspected or known coronary artery disease (CAD) over the past 20 years. Despite its success, the procedure suffers from inefficiency and, at times, inadequate image quality.¹ New developments such as iterative reconstructions with resolution recovery and noise-reduction technology hold promise to improve image quality and reduce acquisition times from that currently recommended by ASNC imaging guidelines.¹⁻³ While image quality may be improved, attenuation artifact still remains and thus attenuation correction should benefit these studies as with full-time acquisitions.

To date, reduced acquisition time with new algorithms has not been evaluated either with attenuation correction imaging techniques or against filtered back-projection (FBP) in a multicenter format. Important SPECT considerations for laboratories considering reduced image acquisition protocols include image quality, interpretive confidence, diagnostic accuracy as well as the extent and severity of perfusion defects and quantitative gated function parameters. The purpose of this investigation was to determine the clinical value of either a standard or shortened protocol using rapid and simultaneous acquisition of both emission and transmission data through examination of these parameters using a new depth-dependent resolution recovery method (Astonish, Philips Medical Systems, Milpitas, CA).

METHODS

Study Design

This study was designed to evaluate qualitative and quantitative parameters comparing images from the same patients using processing methods of standard FBP, full-time Astonish (FTA) processing, and half-time Astonish (HTA) processing. A subsequent phase compared the impact of simultaneously acquired Gd-153 line-source attenuation correction on full-time and half-time Astonish-processed images (FTA-AC and HTA-AC, respectively).

Patients

The patient studies were retrospectively derived from the databases of three SPECT laboratories: 57 patients (30.5%) from Cardiovascular Consultants P.A. (Mid America Heart

Institute, Kansas City, MO), 36 (19.3%) from Hartford Hospital (Hartford, CT), and 94 (50.2%) from Cardiology Associates of Central Connecticut (Wallingford, CT). The studies included consecutive patients from each site that had either (1) a statistical low ($\leq 5\%$) likelihood for CAD according to symptoms, age, gender, and the results of treadmill exercise testing⁴ but excluding the results of SPECT ($n = 55$) or (2) coronary angiography within 181 days (18 ± 30 days) of SPECT with no change in clinical status ($n = 132$). Excluded were patients with (1) percutaneous coronary intervention within 180 days, (2) coronary artery bypass graft surgery, (3) prior cardiac transplantation, and (4) moderate-severe valvular heart disease. Stress testing was performed using treadmill exercise in 58.8%, whereas the remainder underwent either adenosine (Adenoscan, Astellas Pharma, Deerfield, IL) or dipyridamole vasodilator stress alone (32.6%) or vasodilator stress combined with exercise (8.6%). All stress testing was performed in accordance with ASNC procedural guidelines.¹ This study was approved by the Institutional Review Board of each center.

Image Acquisition Protocols

All SPECT studies were acquired using Philips CardioMD small field of view systems with Vantage™ Gadolinium-153 scanning line sources. In accordance with ASNC imaging guidelines,¹ data were acquired over 64 projections at 20-25 seconds per projection for the stress and 30 seconds per projection for the rest images, using a 180° RAO-LPO orbit beginning 15-45 minutes after injection of 10 mCi (rest) and 35 mCi (stress) of Tc-99m sestamibi ($n = 176$) or Tc-99m tetrofosmin ($n = 14$). The collimators were low-energy high resolution, and the energy windows were set at 140 keV \pm 10% for the emission and 100 keV \pm 10% for the Gd-153 line-source transmission data. An additional 118 keV \pm 6% photopeak window was used to compensate for downscatter of Tc-99m into the Gd-153 energy window.^{5,6} All data were acquired using 16-frame ECG gating.

Image Processing

Five rest/stress imaging studies were processed for each patient. The first study was the conventional 64-projection rest/stress image set processed using FBP (Butterworth filter, order 5, critical frequency = 0.45) without attenuation correction. The ECG-gated images were filtered using the same filter except with a critical frequency = 0.35. The second and third studies were rest/stress "full-time" 64-projection data processed with Astonish³ without and with attenuation correction. The transverse images were reconstructed with the OSEM-based Astonish algorithm using four iterations and eight

subsets and a match filter parameter of 1.0. The ECG-gated images were reconstructed with Astonish³ using four iterations, eight subsets and a match filter value of 0.8. The fourth and fifth studies were rest/stress "half-time" Astonish-processed data without and with attenuation correction in which the original 64 projection data were used to generate 32 projections by a "stripping" algorithm that removed every other projection. Therefore, these data sets consisted of 32 projections over 180° that had been acquired for the same time as the 64-projection images. The corresponding ECG-gated images were stripped to 32 projections in the same manner consistent with a 32-projection acquisition. The same approach was applied to the 64-frame transmission projections to produce corresponding simultaneous 32-projection acquisitions. Each projection was normalized to the daily reference scan as with the 64-projection studies. Downscatter correction was applied to each of the 32-transmission projections using the data acquired in the 118 keV ± 6% energy window as with the original 64-projection acquisition.

The transmission maps for the 32- and 64-projection studies were reconstructed using the previously validated method for 64 projections.⁷ The application to 32 projections was described in prior reports.^{8,9} For all attenuation map reconstructions, a uniform initial estimate and 30 iterations of a Bayesian algorithm⁷ applied to the downscatter-compensated projection data was used. Truncation compensation for artifacts occurring in the small field of view transmission images as described earlier¹⁰ was applied to the 32- and 64-projection stress-only images. Attenuation correction was then applied to the Astonish-reconstructed emission images using four iterations and eight subsets and match filter value of 1.0. When applying attenuation correction, Astonish incorporates an attenuation map-based photopeak scatter correction algorithm in addition to the resolution recovery.⁹ Gated images were not attenuation corrected.

Image Interpretation and Scoring

A total of 935 images were interpreted by consensus of two experienced readers. A third reader adjudicated in the <5% cases of discordance of interpretations. The readers were blinded to all clinical information and to the method used for processing the rest/stress images. Readers viewed processed emission and gated images only; the rotating projection images were not made available to avoid potential interpretation bias. Image quality for assessment of both regional perfusion and gated function was interpreted using a 4-point scale of excellent, good, fair, or poor. Fair quality was defined as interpretable, but with sources of image degradation such as suboptimal counts or excessive background activity; poor quality was defined as difficult or impossible to fully interpret because of factors such as very poor count statistics or overlap of portions of the myocardium by adjacent count-rich structures. For analysis, image quality was merged into two categories: excellent/good and fair/poor. Studies were categorized into one of five diagnoses as recommended by ASNC guidelines,¹ after consideration of both regional perfusion and gated function: definitely abnormal, probably abnormal, equivocal, probably normal, and definitely

normal. By use of a standard 17-segment model,¹¹ perfusion at rest and stress for each imaging study was graded on a 5-point scale (0 = normal, 1 = mildly reduced perfusion, 2 = moderately reduced perfusion, 3 = severely reduced perfusion, and 4 = absent perfusion). The visually interpreted segmental scores for each imaging study were added to derive a summed stress score (SSS) and a summed rest score (SRS). A summed difference score was also derived for each imaging study by subtracting the SRS from the SSS. The rest and post-stress gated images (n = 85 and n = 184, respectively) were quantitated for ejection fraction and for both end-diastolic and end-systolic volume using quantitative gated SPECT (QGS, Cedars-Sinai, Los Angeles, CA).

Coronary Angiography

The angiographic reports from each center were submitted to a single investigator who extracted the reported luminal diameter narrowing for the left main and the three major coronary arteries and their major branches. The percentage of luminal narrowing was determined visually. Significant disease was defined at a 70% stenosis threshold in one or more major coronary artery, or 50% stenosis in the left main artery, and this value was used for CAD diagnosis unless otherwise specified.

Statistical Analysis

The power analysis and sample size calculation assumed that a sample size of 171 from a population of 935 would achieve 80% power to detect a difference ($P_0 - P_B$) of 0.037 using a one-sided binomial test, with a target significance level of 0.025. The actual significance level achieved by this test is 0.0222. These results assume a baseline proportion (P_B) of 0.1470 (that for Astonish) and that the actual proportion (P_1) is 0.1765 (that for FBP) based upon a clinically significant difference of 15%.

The results were analyzed in two phases. An initial phase comparing conventional FBP, full-time (FTA), and half-time Astonish (HTA)-processed images without attenuation correction, and a second phase comparing FTA with FTA-AC, HTA with HTA-AC, and FTA-AC with HTA-AC. Comparison was made for quality of both perfusion and gated-function images and for interpretive certainty, using the χ^2 test of independence. All other categorical variables were analyzed with the χ^2 test of independence, McNemar test or Fischer's exact test, as appropriate. For accuracy, definitely normal or definitely abnormal interpretations were used for computations of sensitivity, specificity, whereas probably normal or abnormal and equivocal interpretations were categorized as errors. Summed perfusion scores and quantitative function variables with each processing method were compared using *t*-tests, one-way ANOVA, and the Pearson correlation coefficient. Bland-Altman analysis¹² was used to examine the agreement of post-stress and rest ejection fractions obtained with each processing method. When necessary, post-hoc comparisons were made using the Scheffe test. All analyses were conducted using SPSS Version 15.0 (Chicago, IL, 2006) using a *p*-value of <0.05 as the criterion for statistical significance.

RESULTS

Patients' Demographics

Of 187 eligible patient studies, 78 were female (41.7%). The demographic characteristics of patients are shown comparing the low-likelihood patients with the group that underwent coronary angiography (Table 1). Using a cutoff of $\geq 70\%$ luminal narrowing, coronary angiography revealed that 19% (n = 36) of patients had no significant stenosis, 27% (n = 51) had one-vessel disease, 15.5% (n = 29) had two-vessel disease, and 8.5% (n = 16) had three-vessel disease, including left main disease in this last group. When a cutoff of $\geq 50\%$ luminal narrowing was used to establish CAD significance, 15.5% (n = 29) of patients had no CAD, 18% (n = 33) had one-vessel disease, 22.5% (n = 42) had two-vessel disease, and 15% (n = 28) had three-vessel disease.

First Phase: Evaluation of Filtered Back Projection (FBP) to Full- (FTA) and Half-Time Astonish (HTA)

Image Quality. In comparison with traditional FBP, both FTA and HTA significantly improved image quality for assessment of stress and rest perfusion (Figure 1). The quality of stress acquisitions used for assessment of perfusion was excellent or good in 85% (n = 158), 98% (n = 183), and 95% (n = 178) of

images processed with FBP, FTA, and HTA, respectively ($p < 0.001$). The quality of resting images used for assessment of perfusion was excellent or good in 80% (n = 150), 95% (n = 177), and 92% (n = 172) of images processed with FBP, FTA, and HTA, respectively ($p < 0.001$).

FTA and HTA improved quality of stress images used for functional assessment, whereas quality in rest images was improved by FTA but diminished with HTA in comparison to FBP ($p < 0.01$ for all comparisons, Figure 2). The quality of stress 16-frame gated acquisitions were scored as excellent or good in 89% of images processed with FBP, 98% of FTA images, and 95% of HTA images ($p = 0.002$). Ninety-one patients had resting acquisitions for function assessment. These images were excellent or good in 61, 85, and 41% of images processed with FBP, FTA, and HTA, respectively ($p < 0.001$). All processing methods decreased significantly the quality of the resting function gated images compared to their correspondent stress function images ($p < 0.001$ for all comparisons). In the HTA resting group, 40% of patients had fair and 20% poor images. All of the HTA fair or poor studies were due to low counts except one study with dropped frames due to gating errors.

Representative images are shown in Figures 3 and 4. A patient with a low likelihood of CAD is illustrated in Figure 3A and B. The stress portion is shown in Figure 3A, with FBP in the top panel, FTA in the middle panel, and HTA in the bottom panel. The rest images

Table 1. Comparison of characteristics of low-likelihood and coronary catheterization patients

	Low-likelihood patients	Catheterization patients
N	55	132
Age, years (mean \pm SD)	52 \pm 12	64 \pm 12
Body mass index	29.5 \pm 5.4	31.3 \pm 6.2
Major risk factors, n (%)		
Hypertension	23 (42)	100 (76)
Hypercholesterolemia	27 (49)	100 (76)
Smoking	25 (25)	28 (21)
Family history for CAD	19 (35)	36 (27)
Diabetes mellitus, n (%)	6 (11)	55 (42)
Prior known CAD, n (%)	-	53 (40)
Prior myocardial infarction, n (%)	-	26 (20)
Prior PCI, n (%)	-	45 (34)
Stress test, n (%)		
Exercise	55 (100)	55 (42)
Vasodilator	-	61 (46)
Vasodilator w/Exercise	-	16 (12)

PCI, Percutaneous coronary intervention; CAD, coronary artery disease.

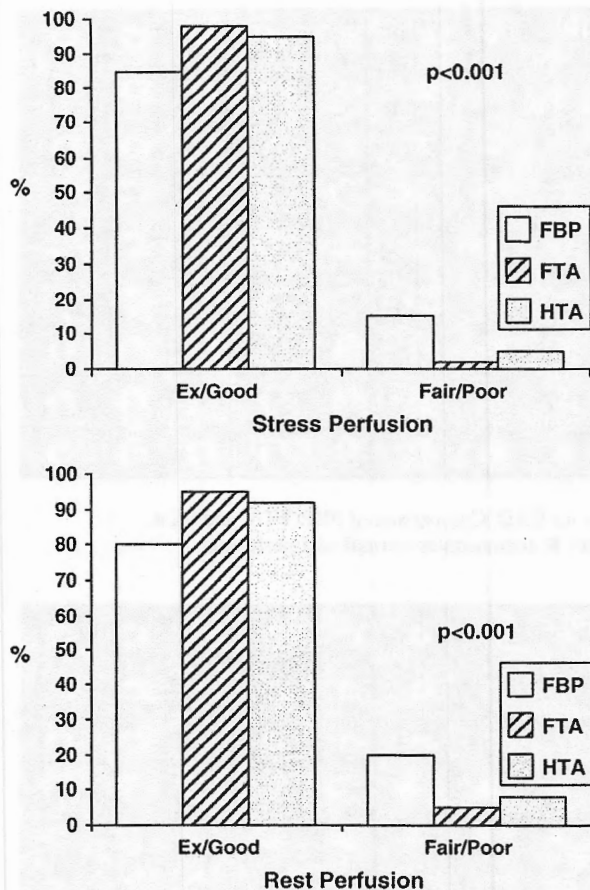


Figure 1. Image quality: stress perfusion (top), rest perfusion (bottom). FBP, Filtered backprojection; FTA, full-time Astonish; HTA, half-time Astonish.

(1/3 dose) are shown in Figure 3B. The image quality was excellent in all three, with normal perfusion.

Images from a 65-year-old male with a history of MI are shown in Figure 4A and B; similar to Figure 3, the top panel is FBP, the middle panel is FTA, and the lower panel is HTA. A medium-sized apical, mid, and basal inferolateral defect is seen at both stress (Figure 4A) and rest (1/3 dosage, Figure 4B), and is fixed. Image quality of the lower dose rest study is also excellent.

Interpretive Certainty. Interpretive certainty of the perfusion images among the various processing methods is shown in Figure 5. Studies were interpreted as definitely normal or definitely abnormal in 89% (n = 166) of FBP images, 83% (n = 155) of FTA images, and 88% (n = 165) of HTA images (p = 0.181).

Diagnostic Accuracy. Diagnostic accuracy was assessed using 70% luminal narrowing. There was no statistically significant difference in diagnostic accuracy between the three processing methods (Figure 6). The

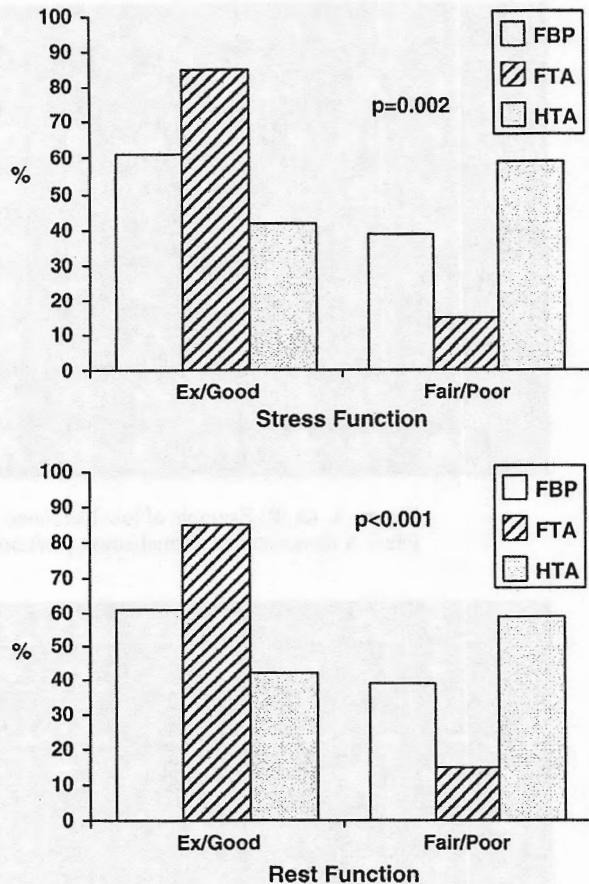


Figure 2. Image quality: stress gating (top), rest gating (bottom). FBP, Filtered backprojection; FTA, full-time Astonish; HTA, half-time Astonish.

normalcy rate of low-likelihood studies (n = 55) that were classified as definitely normal was 91% (n = 50) for FBP images, and 76% (n = 42) for each FTA and HTA images. The differences were not significant (p = 0.079).

Sensitivity, using definitely abnormal interpretations for its calculation, was 76% (73/96), 75% (72/96), and 82% (79/96) for FBP, FTA, and HTA, respectively (p = 0.422). Using definitely normal interpretations to calculate specificity, FBP had a specificity of 75% (68/91), whereas FTA and HTA had specificities of 62% (56/91) and 63% (57/91), respectively (p = 0.113). Sensitivity and specificity rates did not change appreciably when $\geq 50\%$ luminal narrowing was used for diagnosis of CAD with no significant differences observed between the three processing methods.

Perfusion Defect Extent and Severity. There was no statistically significant difference in the summed perfusion scores between the three processing methods, but a trend was noticed for higher scores with both Astonish processing methods. This resulted in a

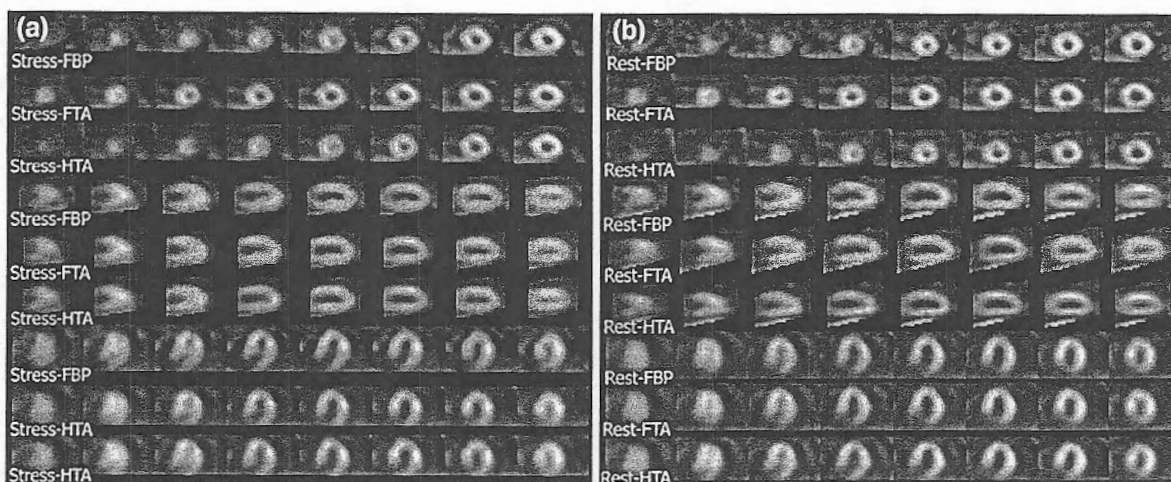


Figure 3. (A, B) Example of low-likelihood patient for CAD. Comparison of FBP, FTA, and HTA. Panel A demonstrates normal stress perfusion. Panel B demonstrates normal rest perfusion.

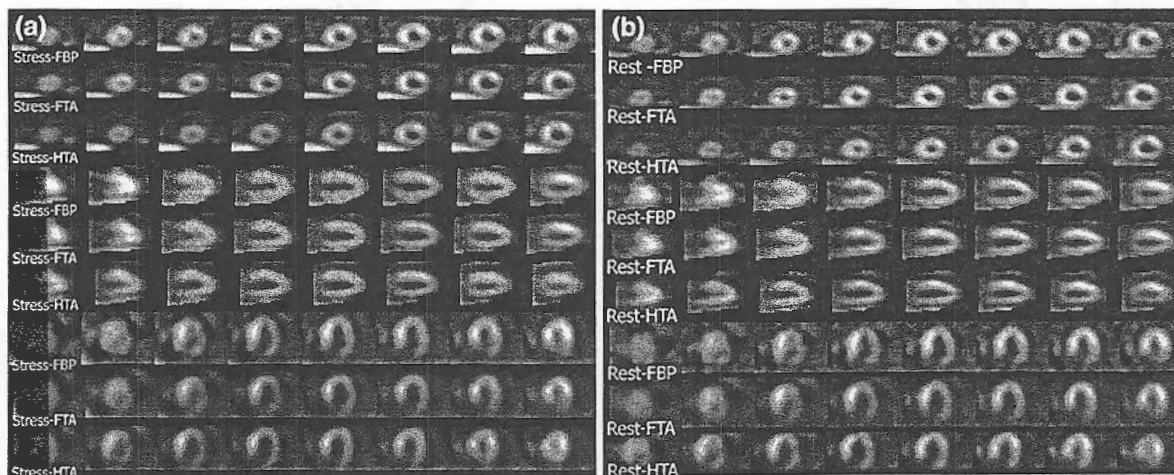


Figure 4. (A, B) Example of a patient with CAD. Comparison of FBP, FTA, and HTA. Panel A demonstrates a medium inferolateral defect at stress. Panel B demonstrates the same medium inferolateral defect at rest.

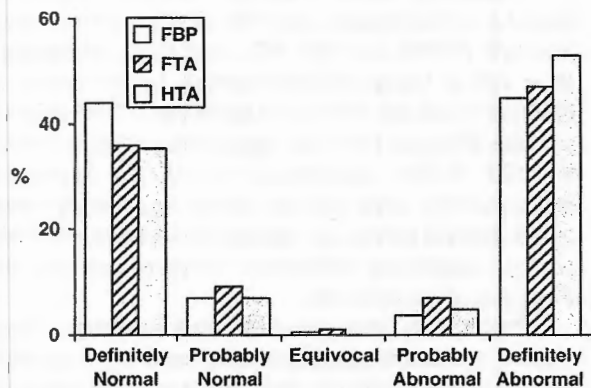


Figure 5. Interpretive certainty. FBP, Filtered backprojection; FTA, full-time Astonish; HTA, half-time Astonish.

marginally significant summed difference score (SDS) when values were separated into SDS ≤ 1 or > 1 (Table 2). A significant linear correlation ($p < 0.001$ for any comparison) was observed between processing methods for the SSS ($r = 0.868-0.919$), SRS ($r = 0.783-0.870$), and SDS ($r = 0.802-0.873$).

Ventricular Function Parameters. Post-stress and rest ejection fractions (EF) were not significantly different between the three processing methods despite a decrease with HTA in resting function image quality (Table 3). Bland-Altman analyses produced small mean differences between the post-stress and rest EF obtained with these processing methods (Table 4). There were no trends in the data favoring one over the other methods. The end-diastolic (EDV) and end-systolic (ESV)

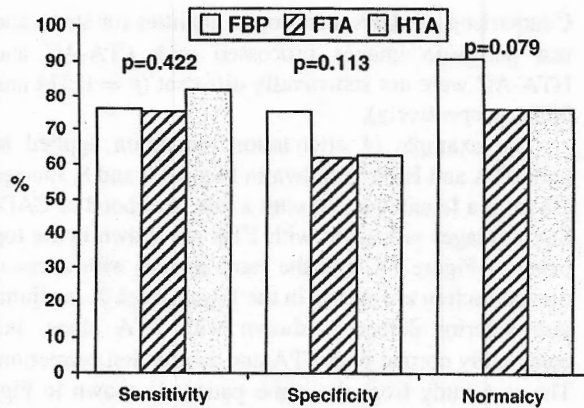


Figure 6. Diagnostic accuracy. *FBP*, Filtered backprojection; *FTA*, full-time Astonish; *HTA*, half-time Astonish.

volumes were also not significantly different (Table 3). A significant linear correlation ($p < 0.001$ for any comparison) was observed between processing methods for post-stress EF ($r = 0.935-0.961$), EDV ($r = 0.930-$

Table 4. Bland-Altman analysis of post-stress and rest ejection fractions obtained from images processed with FBP, FTA, and HTA

	Mean difference	Upper limit	Lower limit
Stress EF FBP – Stress EF FTA	-1.1	5.2	-7.5
Rest EF FBP – Rest EF FTA	-3.1	4.5	-10.8
Stress EF FBP – Stress EF HTA	-0.7	7.3	-8.8
Rest EF FBP – Rest EF HTA	-1.7	6.5	-10

EF, Ejection fraction; *FBP*, filtered backprojection; *FTA*, full-time Astonish; *HTA*, half-time Astonish.

0.960), and ESV ($r = 0.876-0.987$) as well as for rest EF ($r = 0.925-0.961$), EDV (0.909-0.945), and ESV ($r = 0.854-0.959$).

Table 2. Comparison for SPECT perfusion results processed with FBP, FTA, and HTA without attenuation correction (n = 187)

	FBP	FTA	HTA	p-Value
Summed stress score	6.0 ± 7.2	6.9 ± 7.8	7.6 ± 7.8	0.118
SSS 0-3 (n)	50.3% (94)	45.5% (85)	39% (73)	
SSS 4-7 (n)	17.1% (32)	15.5% (29)	18.2% (34)	0.228
SSS >7 (n)	32.6% (61)	39% (73)	42.8 (80)	
Summed rest score	2.0 ± 3.2	1.9 ± 3.6	2.2 ± 3.8	0.728
Summed difference score	4.1 ± 5.7	5.1 ± 6.3	5.5 ± 6.5	0.077
SDS ≤ 1	99 (52.9%)	77 (41.2%)	80 (42.8%)	
SDS > 1	88 (47.1%)	110 (58.8%)	107 (57.2%)	0.047

FBP, Filtered backprojection; *FTA*, full-time Astonish; *HTA*, half-time Astonish; *SSS*, summed stress score; *SDS*, summed difference score.

Table 3. SPECT function results from conventional images processed with FBP compared with FTA and HTA

	FBP	FTA	HTA	p-Value
Post-stress EF (%)	61 ± 11	63 ± 12	62 ± 12	0.640
Post-stress ESV (mL)	42 ± 25	40 ± 26	40 ± 26	0.835
Post-stress EDV (mL)	100 ± 37	98 ± 38	98 ± 38	0.797
Rest EF (%)	63 ± 10	66 ± 11	65 ± 11	0.173
Rest ESV (mL)	39 ± 22	33 ± 23	37 ± 26	0.407
Rest EDV (mL)	99 ± 34	91 ± 35	93 ± 33	0.332
EF Delta (%)	-0.6 ± 5.6	-1.9 ± 5.7	-1.0 ± 7.0	0.384

FBP, Filtered backprojection; *FTA*, full-time Astonish; *HTA*, half-time Astonish; *EF*, ejection fraction; *ESV*, end systolic volume; *EDV*, end diastolic volume. n = 184 for post-stress function values and n = 85 for rest function values.

Second Phase: Evaluation of Attenuation Correction with Astonish Processing

Image Quality. The impact of attenuation correction when applied to FTA and HTA image processing was assessed. The stress images were of excellent or good quality in 98% (183/187) and 93% (173/187) for FTA and FTA-AC, respectively ($p = 0.016$). The resting images were excellent or good in 95% of FTA images (177/187) and 90% (168/187) of FTA-AC images ($p = 0.082$). In the half-time studies, the stress images were of excellent or good quality in 95% (178/187) and 91% (170/187) for HTA and HTA-AC, respectively ($p = 0.104$). The resting perfusion images with excellent or good quality were 92% (172/187) for HTA and 84% (157/187) with HTA-AC ($p = 0.017$).

Comparison of above-mentioned qualities for stress and rest perfusion images processed with FTA-AC and HTA-AC were not statistically different ($p = 0.574$ and 0.092 , respectively).

An example of attenuation correction applied to both FTA and HTA is shown in Figures 7 and 8. Images are from a female patient with a low likelihood of CAD. Stress images processed with FTA are shown in the top panel of Figure 7A, and the same images with attenuation correction are shown in the lower panel. A medium-size anterior defect is shown with FTA alone, but completely normal with FTA and attenuation correction. The rest study from the same patient is shown in Figure 7B using the same format. This study is normal. Image quality of Figure 7A and B is excellent. The same

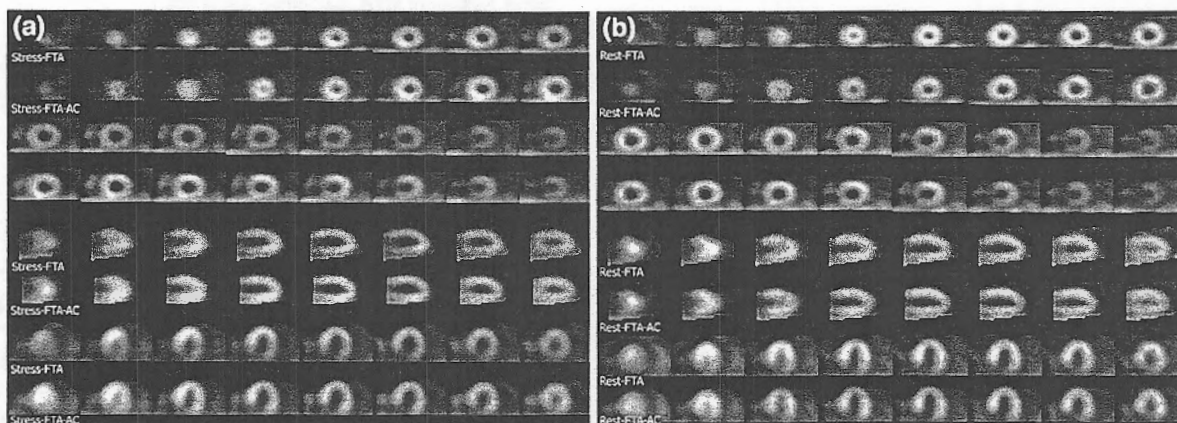


Figure 7. (A, B) Image with full-time Astonish alone and with attenuation correction. The stress image (A) demonstrates an anterior perfusion defect, which with attenuation correction (*lower panel*) becomes normal. The rest study (B) is normal with both.

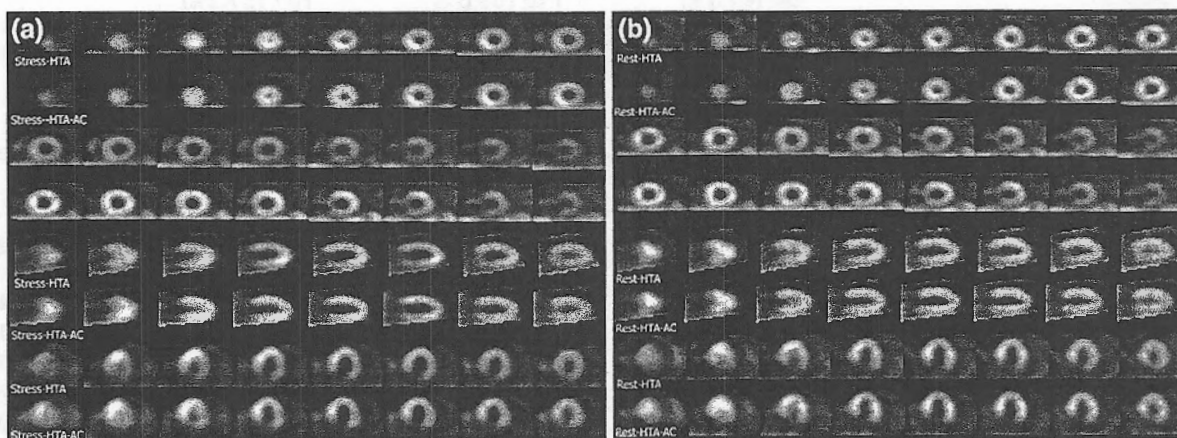


Figure 8. (A, B) Images with half-time Astonish processing alone with stress (A) and with half-time Astonish and attenuation correction. The anterior defect without attenuation correction is shown in the *top panel*, which with attenuation correction is normal. The same patient study at rest is shown in (B), and is normal.

patient study is shown in Figure 8A and B with half-time processing. In Figure 8A, a similar anterior defect is noted in the stress images with HTA alone. This defect is normal in the lower panel with HTA attenuation correction. The rest study (Figure 8B) was normal with HTA for both. Image quality of the rest study, although 1/3 dose, was excellent.

Interpretive Certainty. The percentages of combined definitely normal and abnormal images significantly increased with attenuation correction from 83% (155/187) with FTA and 88% (165/187) with HTA to 97% (181/187) with each FTA-AC and HTA-AC ($p < 0.001$ and 0.004 , respectively). There were only 3% ($n = 6$) of studies interpreted as probably normal ($n = 4$), equivocal ($n = 0$), or probably abnormal ($n = 2$) with either FTA-AC or HTA-AC processing methods (Figure 9). In comparison to FTA, a higher percentage of images with FTA-AC were interpreted as definitely normal (36-44%; $p = 0.005$) and definitely abnormal (47-52%; $p = 0.099$), whereas half-time attenuation correction, when compared to HTA, resulted in a higher percentage of definitely normal interpretations (35-51%; $p < 0.001$) but a lower percentage of definitely abnormal interpretations (53-46%; $p = 0.024$).

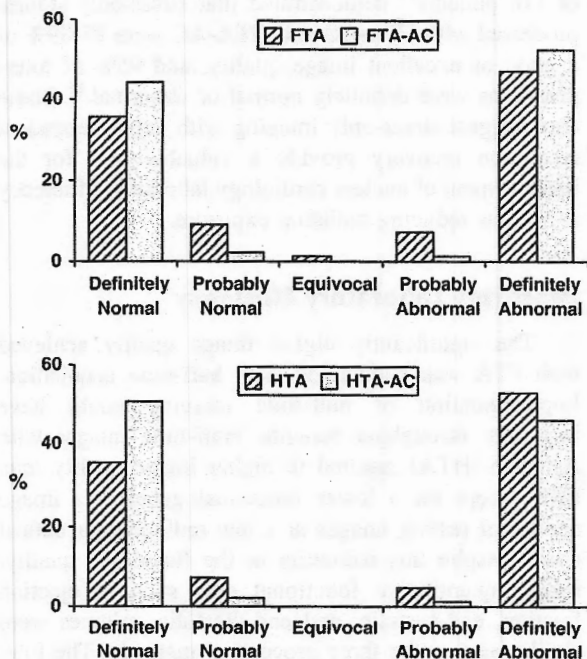


Figure 9. Interpretive certainty. FTA vs. FTA-AC (top), HTA vs. HTA-AC (bottom). FTA, Full-time Astonish without attenuation correction; FTA-AC, full-time Astonish with attenuation correction; HTA, half-time Astonish without attenuation correction; HTA-AC, half-time Astonish with attenuation correction.

Diagnostic Accuracy. Attenuation correction increased significantly the normalcy and specificity rates of FTA and HTA (Figure 10). In the full-time studies, normalcy increased from 76% (42/55) with FTA images to 95% (52/55) with FTA-AC processing method ($p = 0.007$). Specificity also increased from 62% (56/91) with FTA to 78% (71/91) with FTA-AC ($p = 0.015$). The sensitivity increased from 75% (72/96) with FTA to 85% (82/96) with FTA-AC ($p = 0.07$). In the half-time studies, normalcy increased from 76% (42/55) with HTA to 100% (55/55) with HTA-AC ($p < 0.001$). There was no statistically significant difference in normalcy between FTA and HTA with attenuation correction ($p = 0.243$). Specificity increased as well from 63% (57/91) with HTA to 84% (76/91) with HTA-AC ($p = 0.001$). Sensitivity

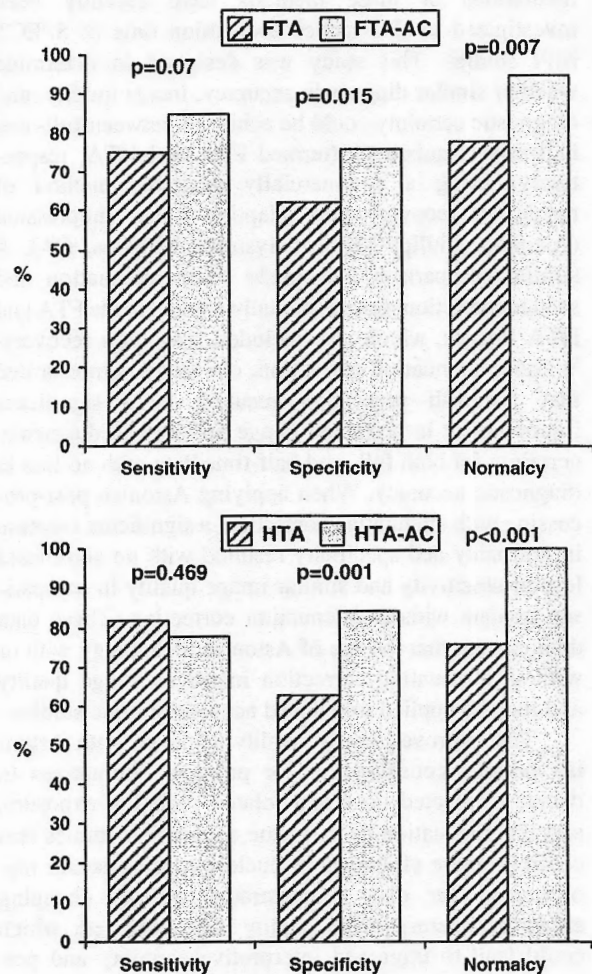


Figure 10. Diagnostic accuracy. FTA vs. FTA-AC (top), HTA vs. HTA-AC (bottom). FTA, Full-time Astonish without attenuation correction; FTA-AC, full-time Astonish with attenuation correction; HTA, half-time Astonish without attenuation correction; HTA-AC, half-time Astonish with attenuation correction.

decreased from 82% (79/96) with HTA to 78% ((75/96) with HTA-AC, although this change was not significant ($p = 0.469$). Comparisons of the diagnostic indices demonstrated no significant differences between FTA-AC and HTA-AC ($p > 0.05$ for all comparisons). Sensitivity and specificity remained similar when $\geq 50\%$ luminal narrowing was used for diagnosis of CAD using either FTA-AC or HTA-AC with no significant differences observed between methods.

DISCUSSION

Recent developments in nuclear cardiology have included post-processing methods such as depth-dependent resolution recovery and iterative reconstruction to improve image quality and accuracy. Various implementations of these methods have recently been investigated to also reduce acquisition time of SPECT MPI studies. This study was designed to determine whether similar diagnostic accuracy, image quality, and diagnostic certainty could be achieved between full- and half-time acquisitions (termed FTA and HTA, respectively) using a commercially available method of resolution recovery and adaptive noise suppression (Astonish, Philips Medical Systems, Milpitas, CA). A similar comparison was made when attenuation and scatter correction was additionally applied to the FTA and HTA images, which also included resolution recovery. Without attenuation correction, our study demonstrated that Astonish processing resulted in a significant improvement in perfusion image quality and diagnostic certainty for both full- and half-time data with no loss in diagnostic accuracy. When applying Astonish post-processing with attenuation correction, a significant increase in normalcy and specificity resulted with no significant loss in sensitivity and similar image quality in comparison to data without attenuation correction. These data demonstrate that the use of Astonish technology with or without attenuation correction improves image quality and may be applied to reduced acquisition time studies.

The improved image quality achieved with Astonish permits consideration for protocol alternatives to decrease injected dose and related radiation exposure, and the application of half-time acquisition studies that could improve efficiency in nuclear cardiovascular laboratories. Our data demonstrated without changing either parameter, image quality was improved, which could lead to improved interpretive certainty and perhaps higher diagnostic accuracy.

Reducing Radiation Exposure

The frequent use of diagnostic and therapeutic procedures requiring ionizing radiation has provided an

increased radiation exposure to patients and has promoted the awareness of an "As Low as Reasonably Achievable" (ALARA) philosophy.¹³ Ionizing radiation causes DNA damage creating concerns for iatrogenic malignancy and heritable genetic defects. Current cardiac imaging studies use a "low dose" of ionizing radiation as described by the BEIR VII report (<100 mSv).¹⁴

Minimizing radionuclide activity (mCi) needed to obtain a good image quality without sacrificing diagnostic accuracy or utilization of stress first/stress-only protocols in appropriate patients is among strategies recommended to minimize radiation exposure to patients undergoing SPECT imaging.¹³ The significantly higher image quality achieved with Astonish-processed images suggests the possibility for studying a lower dose of radionuclide capable of providing a good image quality that would maintain diagnostic certainty and accuracy similar to current levels.

Previous studies have demonstrated that many patients do not need rest imaging,¹⁵ and when combined with attenuation correction reduced the need for rest imaging significantly with no loss in sensitivity ($p < 0.005$).¹⁶ Stress-only MPI reduces radiation exposure by decreasing the effective dose of 9.3-11.3 mSv for a same-day Tc-99m sestamibi or tetrofosmin stress/rest study to an effective dose of 6.6-8 mSv for stress-only studies with same radionuclides.¹³ A recent report of 110 patients¹⁷ demonstrated that stress-only studies processed with FTA-AC and HTA-AC were 87-89% of a good or excellent image quality, and 95% of interpretations were definitely normal or abnormal.¹⁸ These data suggest stress-only imaging with depth-dependent resolution recovery provide a valuable tool for the improvement of nuclear cardiology laboratory efficiency as well as reducing radiation exposure.

Improving Laboratory Efficiency

The significantly higher image quality achieved with FTA was maintained with half-time acquisition. Implementation of half-time imaging could have important throughput benefits. Half-time images with Astonish (HTA) resulted in higher image quality than FBP except for a lower functional gated data image quality of resting images at a low radiopharmaceutical dose. Despite this reduction in the functional quality, resting quantitative functional data such as ejection fraction, end-systolic, and end-diastolic volumes were similar among the three processing methods. The lowered image quality may have been the result of 16-frame gated acquisition rather than 8 frames. The latter procedure was not evaluated in this study, and potentially would provide better image quality. Imaging time can be further reduced if preliminary data on stress-only studies

is confirmed.¹⁷ The reduction in imaging time translates in less discomfort to patients, lesser opportunity for patient motion, and an improved laboratory throughput.

Reduced acquisition time SPECT MPI is not unique to the technology used in this article. DePuey et al compared another ordered subset expectation maximization (OSEM) resolution recovery and "wide beam reconstruction" (WBR) with images processed also with FBP methods.¹⁹ Results from this study suggest that image quality was preserved with a half-time acquisition from either method of processing, although WBR was preferred. Ali et al compared half-time with full-time gated myocardial SPECT images also processed with ordered-subset expectation maximization with resolution recovery (OSEM-RR), with and without CT-based attenuation correction.²⁰ Results from this study showed significant correlations ($p < 0.01$) between the half-time and full-time images for summed perfusion scores, regional wall motion, left ventricular volumes, ejection fraction, and dilation. In contrast to these studies, ours was a multicenter study and assessed the diagnostic accuracy of each processing method by comparing the imaging diagnostic interpretation with coronary angiography findings.

Attenuation Correction

The second phase of this study examined the impact of attenuation correction upon Astonish imaging. An important finding was that of improved normalcy and specificity for both full-time and half-time Astonish data, with no loss in sensitivity. These data demonstrate that attenuation correction adds to the information provided by the depth-dependent resolution recovery, consistent with multiple previous studies demonstrating improved specificity using line-source attenuation correction devices.¹⁴ Based on clinical context, these data suggest that the ideal use of depth-dependent resolution recovery algorithms should be performed in conjunction with a validated form of attenuation correction.

Limitations

Our approach removed every other projection from the rest and stress clinically indicated 64-projection emission studies, and the transmission projections to create "equivalent" 32-projection studies. This was justified based largely on the negligible myocardial redistribution of the Tc-99m perfusion agents. Additionally, we made the assumption that any changes in extracardiac activity that might affect the images, in particular subdiaphragmatic activity, would not impact the reconstruction. It is, however, possible that in the clinical acquisition of 32-projection studies, where the

acquisition time is one-half the conventional imaging times, there may be a change in the distribution of patient motion from conventional studies. In processing our studies when motion correction was required, there was not a noticeable difference in the ability to correct the projection images between 32- and 64-projection studies.

The accuracy of attenuation maps created from 32-projection studies was investigated in an earlier study and shown that accurate maps could be obtained for count levels that would exceed the lower limits expected in these studies. Each attenuation map was reviewed at the time of processing and no maps were found to have unacceptable image quality and were thus included in the processing. While it was not specifically evaluated, errors in the performance of truncation compensation as described in an earlier publication was not observed for either 32- or 64-projection studies.

This study was conducted to provide diagnostic accuracy data. As such, patient studies that had imaging procedures from three laboratories and subsequently underwent cardiac catheterization were selected for evaluation in addition to low-likelihood patients. This study was not prospective. As a result, the "half-time acquisition" was analyzed by "data stripping" of every other projection. Therefore, this was not a true half-time acquisition. While a potential limitation, true half-time acquisition may have resulted in less motion artifact due to less time. Thus, this method potentially disadvantaged the half-time data.

CONCLUSION

Depth-dependent resolution recovery using the Astonish algorithm results in improved image quality for both full-time and half-time acquisitions when compared to standard FBP processing, without a loss in diagnostic accuracy. The addition of line-source attenuation correction resulted in similar image quality and improved specificity and normalcy, suggesting the optimal method should include both procedures.

References

1. American Society of Nuclear Cardiology. Imaging guidelines for nuclear cardiology procedures. *J Nucl Cardiol* 2006;13(6):e25-171.
2. Borges-Neto S, Pagnanelli RA, Shaw LK, Honeycutt E, Shwartz SC, Adams GL, et al. Clinical results of a novel wide beam reconstruction method for shortening scan time of Tc-99m cardiac SPECT perfusion studies. *J Nucl Cardiol* 2007;14(4):555-65.
3. Ye J, Song X, Zhao Z, Da Silva AJ, Weiner JS, Shao L. Iterative SPECT reconstruction using matched filtering for improved image quality. In: IEEE nuclear science symposium conference record, 29 Oct-1 Nov 2006, San Diego, CA; 2006. p. 2285-7.

4. Diamond GA, Forrester JS. Analysis of probability as an aid in the clinical diagnosis of coronary-artery disease. *N Engl J Med* 1979;300(24):1350-8.
5. Henzlova MJ, Cerqueira MD, Mahmarian JJ, Yao SS. Stress protocols and tracers. *J Nucl Cardiol* 2006;13(6):e80-90.
6. Case JA, Cullom SJ, Bateman TM. Myocardial perfusion SPECT attenuation correction. In: Iskandrian AE, Verani MS, editors. *Nuclear cardiac imaging: principles & applications*. New York: Oxford University Press; 2002.
7. Case JA, Hsu BL, Bateman TM, Cullom SJ. A Bayesian iterative transmission gradient reconstruction algorithm for cardiac SPECT attenuation correction. *J Nucl Cardiol* 2007;14(3):324-33.
8. Cullom SJ, Krishnendu S, Hsu B. Downscatter compensation for attenuation correction with rapid 32-angle simultaneous Tc-99m emission-gadolinium-153 transmission scanning. *J Nucl Cardiol* 2007;14(Suppl 1):S98.
9. Cullom SJ, Saha K, Case JA. Accurate reconstruction of rapidly acquired 32-angle Gd-153 scanning line source transmission projections for myocardial perfusion SPECT attenuation correction. *J Nucl Cardiol* 2007;14(Suppl 1):S98-9.
10. Noble GL, Ahlberg AW, Kokkiralala AR, Cullom SJ, Bateman TM, Cyr GM, et al. Validation of attenuation correction using transmission truncation compensation with a small field of view dedicated cardiac SPECT camera system. *J Nucl Cardiol* 2009;16(2):222-32.
11. Cerqueira MD, Weissman NJ, Dilsizian V, Jacobs AK, Kaul S, Laskey WK, et al. Standardized myocardial segmentation and nomenclature for tomographic imaging of the heart: A statement for healthcare professionals from the Cardiac Imaging Committee of the Council on Clinical Cardiology of the American Heart Association. *Circulation* 2002;105(4):539-42.
12. Bland JM, Altman DG. Statistical methods for assessing agreement between two methods of clinical measurement. *Lancet* 1986;1(8476):307-10.
13. Einstein AJ, Moser KW, Thompson RC, Cerqueira MD, Henzlova MJ. Radiation dose to patients from cardiac diagnostic imaging. *Circulation* 2007;116(11):1290-305.
14. Committee to Assess Health Risks from Exposure to Low Levels of Ionizing Radiation NRCotNA. *Health risks from exposure to low levels of ionizing radiation: BEIR VII Phase 2*. Washington, DC: The National Academies Press; 2006.
15. Schroeder-Tanka JM, Tiel-van Buul MM, van der Wall EE, Roolker W, Lie KI, van Royen EA. Should imaging at stress always be followed by imaging at rest in Tc-99m MIBI SPECT? A proposal for a selective referral and imaging strategy. *Int J Card Imaging* 1997;13(4):323-9.
16. Heller GV, Bateman TM, Johnson LL, Cullom SJ, Case JA, Galt JR, et al. Clinical value of attenuation correction in stress-only Tc-99m sestamibi SPECT imaging. *J Nucl Cardiol* 2004;11(3):273-81.
17. Bateman TM, Heller GV, McGhie AI, Courter SA, Kennedy KF, Katten D, et al. Application of simultaneous Gd-153 line source attenuation correction to half-time stress only SPECT acquisitions: A multicenter clinical evaluation. *J Am Coll Cardiol* 2008;51(Suppl A):A171.
18. Thompson RC, Heller GV, Johnson LL, Case JA, Cullom SJ, Garcia EV, et al. Value of attenuation correction on ECG-gated SPECT myocardial perfusion imaging related to body mass index. *J Nucl Cardiol* 2005;12(2):195-202.
19. DePuey EG, Gadiraju R, Clark J, Thompson L, Anstett F, Shwartz SC. Ordered subset expectation maximization and wide beam reconstruction "half-time" gated myocardial perfusion SPECT functional imaging: A comparison to "full-time" filtered back-projection. *J Nucl Cardiol* 2008;15(4):547-63.
20. Ali I, Ruddy TD, Almgrahi A, Anstett FG, Wells RG. Half-time SPECT myocardial perfusion imaging with attenuation correction. *J Nucl Med* 2009;50(4):554-62.